

Submitted to *The Astronomical Journal*

Intrinsic Narrow Absorption Lines in HIRES/Keck Spectra of a Sample of Six Quasars¹

Rajib Ganguly, Michael Eracleous, Jane C. Charlton ², and Christopher W. Churchill ³

Department of Astronomy and Astrophysics
 The Pennsylvania State University, University Park, PA 16802
 e-mail: `ganguly, mce, charlton, cwc@astro.psu.edu`

Submitted to *The Astronomical Journal*

ABSTRACT

In the course of a large survey of intervening MgII absorbers in the spectra of quasars, the CIV emission lines of six of the target objects (three radio-loud and three radio-quiet) were observed serendipitously. In four of these six quasars, we detected “associated” narrow absorption lines with velocities within 5000 km s^{-1} of the quasar emission-line redshift (three of these four quasars are radio-quiet while the other is radio-loud). As a result of the original target selection, the small sample of six quasars is unbiased towards finding associated absorption lines. In three of these four cases, the absorption line optical-depth ratios deviate from the prediction based on atomic physics, suggesting that the background photon source(s) are only partially covered by the absorbing medium and, by extension, that the absorption lines are intrinsic to the quasar. We have used the method of Barlow & Sargent to determine the effective coverage fraction of background source(s) and we have extended it to constrain the coverage fraction of the continuum and broad-emission line sources separately. We have also applied this refined method to the narrow intrinsic absorption lines in three additional quasars for which the necessary data were available from the literature. We find that in two objects from our sample, the *continuum* source must be partially covered regardless of the covering factor of the emission-line source. We discuss these results in the context of the properties of absorption lines observed in different types of active galaxies and related outflow phenomena. We cannot distinguish between possible mechanisms for

¹Based in part on observations obtained at the W. M. Keck Observatory, which is jointly operated by the University of California and the California Institute of Technology.

²Center for Gravitational Physics and Geometry, The Pennsylvania State University

³Visiting Astronomer, The W. M. Keck Observatory

the origin of the partial coverage signature although we do consider possible observational tests. Finally, we speculate on how the gas responsible for the narrow lines may be related to the accretion disk wind that may be responsible for the broad absorption lines observed in some quasars.

Subject headings: quasars: absorption lines — quasars: individual (Q 0450 – 132, Q 1213 – 003, PG 1222 + 228, PG 1329 + 412)

1. Introduction

Absorption by an ionized medium close to the central engine is now recognized as a fairly common feature in the spectra of active galactic nuclei (hereafter AGNs). In Seyfert 1 galaxies, the signature of the ionized gas takes the form of narrow UV resonance absorption lines from highly-ionized species, such as Nv and CIV (Crenshaw, Maran, & Mushotzky 1998) as well as soft X-ray absorption edges from highly ionized species such as OvII and OvIII (Reynolds 1997; George et al. 1998). Similar UV absorption lines⁴ are also observed in quasars (e.g. Foltz et al. 1986; Anderson et al. 1987; Young, Sargent, & Boksenberg 1982; Sargent, Boksenberg, & Steidel 1988; Steidel & Sargent 1991). Quasars, however, are perhaps better known for their *broad* absorption lines, whose widths often reach 50,000 km s⁻¹ (e.g., Turnshek et al. 1988; Weymann et al. 1991). The high ionization state of the absorbers and the often blueshifted absorption lines (relative to the broad emission lines) suggest that the absorber is a fairly tenuous medium outflowing from the AGN, most likely accelerated by radiation pressure (Arav et al. 1995). The absorber could plausibly be associated with an accretion–disk wind (e.g., Murray et al. 1995; Krolik & Kriss 1995) analogous to those observed in many cataclysmic variables (e.g., Drew 1990; Mauche et al. 1994). This can only be a broad analogy, however, since a number of observational clues suggest that the picture in AGNs is neither as simple nor as “clean” as in cataclysmic variables. For example, the fact that absorption line depths often exceed either the net continuum level or the net emission–line level on which they are superposed suggests that the absorber does not lie between the broad emission–line region (BELR) and the more compact continuum source since it intercepts both continuum and emission–line photons. That is, it lies either within the BELR or away from both regions.

The relation between the absorption–line region and the ubiquitous AGN emission–line regions is unknown, although it has been suggested that they may represent different phases or layers of the same medium (Shields, Ferland, & Peterson 1995; Hamann et al. 1998). From an observational perspective, it is important to determine the geometry of the absorbing gas and its physical conditions because these constitute useful constraints on theoretical models of the ionization and

⁴Here, we consider only absorption lines which are close to the redshift of the quasar, i.e. $z_{\text{abs}} \approx z_{\text{em}}$, not lines at considerably lower redshifts than that of the quasar.

acceleration of the outflow. Moreover, it is also interesting to ask whether there are any trends in the properties of the absorption lines with AGN subclass since such trends serve as constraints on scenarios of fundamental differences between such subclasses (e.g., the radio-loud/radio-quiet AGN dichotomy). It is, therefore, encouraging that some progress has been made in recent years in answering the above questions. First, observations of large samples of quasars indicate that *broad* absorption lines (BALs) are found preferentially among radio-quiet quasars (Stocke et al. 1992), while the preferred hosts of associated⁵ *narrow* absorption lines (NALs) are radio-loud quasars (Foltz et al. 1986; Anderson et al. 1987). These trends are by no means well-established and have been called into question by the discovery of radio-loud BAL quasars (Becker et al. 1997; Brotherton et al. 1998) and radio-quiet intrinsic NAL quasars (Hamann, Barlow, & Junkkarinen 1997a; Hamann et al. 1997b). We note, however, that the Foltz et al. (1986) and Anderson et al. (1987) results discuss the preference of *strong* associated NALs for radio-loud quasars, while also demonstrating that weak associated NALs occur in both radio-quiet and radio-loud quasars. Second, observations of selected NAL quasars at high spectral resolution have shown that the absorbers only partially cover the background BELR and/or continuum source (Barlow & Sargent 1997; Hamann et al. 1997a). In another quasar, the NALs were found to vary on a time scale of only a few months (Hamann et al. 1997b). These observations demonstrate that the NALs in these objects are intrinsic and also provide useful constraints on their geometry.

In this paper, we present five associated NALs along the lines of sight toward six quasars observed at high spectral resolution. These were discovered serendipitously in a survey of *intervening* Mg II absorbers ($z_{\text{abs}} \ll z_{\text{em}}$; Churchill 1997). In three of the five cases, the NAL systems exhibit the partial coverage signature of absorbing gas *intrinsic* to the quasar. In the process of analyzing the data, we have refined and expanded the method of Barlow & Sargent (1997) to treat the coverage fractions of the continuum source and the BELR separately. Although it is, in principle, impossible to determine the two coverage fractions independently using an absorption doublet, it is possible to place interesting constraints on them. In particular, we find that in two of the quasars in this small collection, the continuum source must be partially covered by the absorber.

In §2 of this paper, we describe the selection of the original quasar sample, the observations and data reduction, and the properties of the associated NALs that we detected and other relevant properties of their hosts. In §3 and §4, we show that, in three of these systems, the relative strengths of the absorption lines provide evidence for partial coverage of the background source by the absorber. In §4, we determine the effective coverage fractions by applying the method of Barlow & Sargent (1997). We also develop and apply a refined version of this method in which we treat the coverage fraction of the continuum source and broad BELR separately. In §5, we discuss the implications of the observational results, possible partial coverage mechanisms, and the general

⁵“Associated” absorption lines, according to the definition of Anderson et al. (1987), are those with velocities within 5000 km s^{-1} of the quasar rest frame. In principle, associated absorption lines need not be intrinsic to the quasar.

picture of intrinsic absorbers in different types of active galaxies. In §6, we summarize our findings and present our final conclusions.

2. Sample of Objects, Observations, and Data

The associated NAL systems reported here were found in the course of a large statistical study of intervening MgII absorbers during which spectra of a sample of 25 quasars were obtained (Churchill 1997). In six objects from this sample, the spectra included the broad CIV emission line and revealed the presence of five associated NAL systems within 5000 km s^{-1} of the emission-line redshift. Another system at $\Delta v = -13,800 \text{ km s}^{-1}$ toward Q 0450 – 132 could be “associated” (see Petitjean, Rauch, & Carswell 1994), but it does not satisfy the traditional velocity criterion. These six quasars are listed in Table 1 along with the some of their basic properties. The emission redshifts and emission line fluxes for the quasars were taken from Sargent et al. (1988) and from Steidel & Sargent (1991). Because of the way the original sample was selected, the final collection of six quasars whose CIV emission lines were observed is unbiased towards the presence of associated CIV NALs. In two of the six objects the spectra include additional absorption lines, namely SiIV and Nv in Q 0450 – 132 and SiIV in Q 1213 – 003.

Since the radio properties of these quasars are important to our later discussion, we have compiled information about their radio properties based on reports in the literature and included it in Table 1 along with the appropriate references. The observed 5 GHz radio flux was converted to the rest frame of the source using the measured spectral index α , if available, or assuming $\alpha = 0.5$ otherwise (where $f_\nu \propto \nu^{-\alpha}$). The radio power was computed assuming a Hubble constant of $50 \text{ km s}^{-1} \text{ Mpc}^{-1}$, and a deceleration parameter of $\frac{1}{2}$, following Kellermann et al. (1994). The rest-frame 4400 Å optical flux was calculated from the observed V magnitude assuming a flat optical–UV spectrum (i.e., $\alpha = 0$; Elvis et al. 1994). To classify an object as radio–loud or radio–quiet, we adopted the criteria of Kellermann et al. (1994) according to which radio–loud quasars have either a 5 GHz power of $P_{5 \text{ GHz}} > 10^{26} \text{ W Hz}^{-1}$ or a 5 GHz–to–4400 Å flux density ratio of $R > 10$. According to these criteria, three of the six objects are radio–quiet and three are radio loud.

The observations were carried out with the HIRES spectrometer (Vogt et al. 1994) on the Keck I telescope. The spectra have a resolution of 6.6 km s^{-1} with a sampling rate of 3 pixels per resolution element. They were reduced with the IRAF⁶ `apextract` package for echelle data. The detailed steps for the reduction are outlined in Churchill (1997).

The details of the observations are listed in Table 2 which also includes the parameters of the associated NAL systems that we detected along with the lowest measurable equivalent widths (5σ

⁶IRAF is distributed by the National Optical Astronomy Observatories, which are operated by AURA, Inc., under contract to the NSF.

limits) in the corresponding spectrum. In this table, we give the mean velocity of each absorption-line system relative to the peak of the broad emission line. NALs were found at both negative (blueshifted) and positive (redshifted) velocities relative to the CIV broad emission-line peak. A positive velocity, such as seen in PG 1222 + 228 and PG 1329 + 412, need not imply infall toward the quasar since the true velocity of the quasar is more accurately measured by narrow forbidden lines than by the broad emission line peaks. For example, in a picture in which the NAL gas is outflowing from the central engine, the NAL redshift would imply a smaller outflow velocity of the absorbers relative to the broad emission-line gas.

Figures 1–5 present the velocity aligned absorption profiles of the CIV doublets and of other detected transitions (SiIV and Nv) of the five associated systems that were covered in the HIRES/Keck I spectra. The CIV λ 1550 profile of the $\Delta v = -60$ km s $^{-1}$ system of Q 1213 – 003 (Figure 3) is truncated near 0 km s $^{-1}$ because it falls off the edge of the CCD. In fact, because of the redshift of Q 1213 – 003 its CIV emission line is in the observed wavelength range above 5100 Å, where the echelle orders are separated by gaps. As a result, there are several gaps in the coverage of the broad emission-line profile. None of the other objects suffer from this problem, however.

The kinematic structure of the NAL profiles is varied and has multiple components. It is not distinguishable from the structure found in intervening absorbers. However, the strong Nv absorption in Q 0450 – 132 is indicative of the typically high metallicities of associated systems (Petitjean et al. 1994) in contrast to the lower metallicities of intervening systems. In §3 and §4, we demonstrate that in three of the five systems there is evidence that the absorbing clouds only partially cover the source, which then requires them to be in relatively close proximity to the source. It should be noted that the $\Delta v = -60$ km s $^{-1}$ system of Q 1213 – 003 has been classified as intrinsic by Sowinski, Schmidt, & Hines (1997), but we have not been able to find the relevant report in the literature.

3. Identification of Anomalous Optical Depths

In the three of the quasars displaying NALs we find that the optical depth ratio of the two members of the CIV doublet did not have the value expected from atomic physics, namely $\frac{\tau_1}{\tau_2} = \frac{f_1\lambda_1}{f_2\lambda_2}$ (Savage & Sembach 1991; where f_1 and f_2 are the oscillator strengths and λ_1 and λ_2 are the rest wavelengths of the doublet members). To demonstrate this discrepancy, we have fitted the weaker member of each doublet with a combination of Voigt profiles, scaled the model according to what atomic physics dictates for the stronger member of the same doublet, and compared it to the data. The results of this exercise are illustrated in Figures 1–5, where we show the models as solid lines superposed on the data. The bottom panel in each set shows the deviation of the data from the predicted profile of the strongest member of each doublet in each resolution element, scaled by the error bar. We see three obviously discrepant cases: the $\Delta v = -2011$ km s $^{-1}$ system toward Q 0450 – 132 (Figure 1), the $\Delta v = +1482$ km s $^{-1}$ system toward PG 1222 + 228 (Figure 4), and the $\Delta v = +314$ km s $^{-1}$ system toward PG 1329 + 412 (Figure 5). Neither of the associated systems

toward Q 1213 – 003 appear to deviate from the atomic physics prediction.

We consider five explanations for the apparent violation of the optical depth scalings in these three associated systems: (1) an instrumental/reduction effect such as scattered light which mimics a source function (e.g., Crenshaw et al. 1998) (2) blends with other transitions at other redshifts; (3) a source function that fills in the line cores (Wampler, Chugai, & Petitjean 1995); (4) incomplete occultation of the continuum and/or emission-line by the absorbers (Wampler, Bergeron, & Petitjean 1993; Wampler et al. 1995; Hamann et al. 1997a,b; Barlow & Sargent 1997) and (5) scattering of background photons back into the light path. The first is an unlikely resolution to the problem since the optical depth scaling is obeyed by all 64 intervening absorption-line systems (including transitions from CIV, MgII, and FeII) observed with the same instrumental setup and reduced in the same manner (Churchill et al. 1998). In addition, we have searched the spectra of these quasars for an extensive set of transitions at the redshifts of all other known systems, and found that none of them affect the profiles studied here. This rules out the second possibility. Some forms of the source function explanation could be viable while others are not; we consider these further in §5.2. The fourth and fifth explanations have identical signatures, since we can think of scattering as a form of “effective partial coverage”. Intuitively, the partial coverage effect will cause models that assume full coverage to over-predict the strength of the stronger member of a doublet, relative to the weaker. Physically, the intensity observed in the core of an absorption profile is the composite of two types of light paths: (1) light that is not occulted by the absorbing clouds or is scattered back into the light path, and (2) the light that successfully passes through the absorbers. The unocculted fraction (in normalized units) is nearly the same for both members of the doublet provided the emission line is not too steep over the wavelength range covered by the absorption (see Appendix). This results in a larger increase in the flux, relative to the full coverage expectation, detected in the deeper blue member of the doublet relative to the red member. The most straightforward example is a situation in which the absorbers are optically thick such that the unattenuated flux is negligible at either member of the doublet. With partial coverage, one still observes a significant flux which is equal in the two members.

4. Partial Coverage

4.1. Effective Coverage Fraction C_f

To pursue the partial coverage interpretation further we have computed the effective coverage fraction following Barlow & Sargent (1997) and Hamann et al. (1997a). The effective coverage fraction is computed by considering the fraction of all photons of a given wavelength that do not pass through the absorbing gas. This calculation assumes a single, *extended* continuum and emission-line source and a single effective optical depth appropriate to the absorbing clouds at the corresponding velocity. If τ is the effective optical depth of an absorbing cloud that occults a

fraction C_f of the source, the observed residual intensity, R , in normalized units is:

$$R(\lambda) = [1 - C_f(\lambda)] + C_f(\lambda)e^{-\tau(\lambda)} . \quad (1)$$

The first term on the right-hand side represents the photons traveling along unocculted lines of sight while the second term arises from photons that survive absorption due to the finite optical depth of the cloud.

For two multiplet transitions, the conjunction of the two residual intensities with the optical depth scaling yields the coverage fraction through the solution to:

$$\left[\frac{R_r - 1 + C_f}{C_f} \right]^{\frac{f_b \lambda_b}{f_r \lambda_r}} = \frac{R_b - 1 + C_f}{C_f} , \quad (2)$$

where the subscripts “r” and “b” refer to the properties of the redder and bluer transitions, respectively. For the resonant UV doublets, such as CIV $\lambda\lambda 1548, 1550$, $\frac{f_b \lambda_b}{f_r \lambda_r} \approx 2$ allowing an analytic solution:

$$C_f(v) = \frac{[R_r(v) - 1]^2}{R_b(v) - 2R_r(v) + 1} , \quad (3)$$

where we have converted the wavelength dependence of the coverage fraction to a velocity dependence. In the application of this method to the data, the calculation of C_f was performed in each resolution element along each of the resonant doublet profiles for the three associated systems with anomalous optical depth ratios. The results are illustrated as points with 1σ error bars in the bottom window of each panel of Figures 6–8. Points are only plotted if: (1) the stronger transition is detected, using the aperture method (Lanzetta, Turnshek, & Wolfe 1987), at the 3σ level; (2) the derived coverage fraction is physical ($0 < C_f < 1$); (3) the 1σ error in C_f , $\sigma_{C_f} < 0.5$; and (4) the fractional uncertainty in C_f is less than unity.

A notable trend is that the coverage fraction always drops toward the wings of lines. This is an effect of the instrument’s line spread function which tends to “wash out” the wings and artificially cause anomalous optical depth ratios. We have explored this effect by simulating observed spectra with normal optical depth ratios and analyzing them in the same way as the data. As shown in Figure 9, synthetic spectra which are not convolved with the line spread function exhibit no variation in the coverage fraction across the single component Voigt profile. When convolved with the instrumental resolution function, even a profile with $C_f = 1$ will show $C_f < 1$ in its wings due to this convolution effect. The signal-to-noise ratio of the observed spectra was not high enough to merit an attempt to deconvolve the line spread function. Therefore it is only possible to interpret the derived C_f values in the cores of well-resolved lines.

There is evidence for partial coverage ($C_f < 1$) over a significant range of velocity for the three systems. The values of C_f , averaged over the velocity regions defined by the *apparent* location of kinematic components in the profile, are given in Table 3. The weighted mean values of C_f , averaged over all resolution elements in the regions, are also shown graphically in the top windows of Figures 6–8, where they are represented by the level of the horizontal bars. The width of the

horizontal bars depicts the velocity bin over which the average value of C_f was computed. (Note that the vertical bar does not represent an error bar but rather it indicates the coverage fraction derived separately for the BELR, as discussed in the next section.)

We have also found that the effective coverage fraction varies with velocity component, as follows. In the case of Q 0450 – 132 (Figure 6), the spectrum includes absorption lines from three species, CIV, SiIV, and Nv. The coverage fraction was derived in five separate regions of the CIV profile and there is evidence that it varies from component to component. The Nv data are noisy, but consistent with the coverage fraction derived for CIV in regions of overlap. The $\Delta v = -2100 \text{ km s}^{-1}$ component that shows strong SiIV absorption (presumably originating from a lower-ionization region of the absorber) also shows partial coverage consistent with the corresponding component of CIV. There are two distinct components in the PG 1222+228 intrinsic CIV absorption profile (Figure 7), both of which yield a small coverage fraction: the $\Delta v = +1469 \text{ km s}^{-1}$ component gives $C_f \approx 0.7$ while the $\Delta v = +1587 \text{ km s}^{-1}$ component gives a coverage fraction of about $C_f \approx 0.4$. The effective coverage fraction was also determined in four separate regions of the intrinsic CIV profile of PG 1329 + 412 (Figure 8); in two of which we found $C_f < 1$.

4.2. Partial Coverage of Continuum and Emission Line Sources

The single number C_f gives the fraction of all photons at a given wavelength that pass through absorbers along the line of sight. However, at the position of these associated absorption lines in the spectrum, the absorbed photons have two significant sources, the continuum source and the BELR. The continuum source is likely to be significantly smaller than the BELR, but the geometry and relative position of the BELR is unknown. In this section, we continue to assume that the photons from these two regions pass through the same absorbers, i.e. that the optical depth τ is the same along the paths to the observer from the continuum source and from the BELR. However, we now consider the different coverage fractions, C_c and C_{elr} , that can apply for the continuum source and the BELR. First we define, $W = F_{\text{elr}}/F_c$, as the ratio of the broad emission-line flux to the continuum flux at the wavelength of the narrow absorption line. Then we can write the normalized flux as:

$$R = 1 - \frac{(C_c + WC_{\text{elr}})(1 - e^{-\tau})}{(1 + W)} . \quad (4)$$

By the same optical depth scaling argument as in the previous section, this reduces down to:

$$\frac{C_c + WC_{\text{elr}}}{1 + W} = \frac{[(R_r(v) - 1)]^2}{R_b(v) - 2R_r(v) + 1} = C_f , \quad (5)$$

where we have assumed that underlying, unabsorbed continuum plus line flux is the same in both transitions, i.e., that the value of W is the same for both members of the doublet. In the Appendix we calculate that C_c or C_{elr} will change by at most 15% if a doublet is on the steep slope of an emission line due to a differing W . Equation (5) shows that the effective coverage fraction, C_f , can be considered as an average coverage fraction weighted according to the flux from each source.

Of course, with the available information, the continuum source and BELR coverage fractions cannot be determined independently of each other. It is possible, nevertheless, to place interesting constraints on them. Given the value of C_f and W , and their 1σ uncertainties, equation (5) defines a region in the C_c – C_{elr} parameter plane where the solution must lie. Examples of such regions are illustrated in Figure 10. It is interesting to note that, if the upper boundary of this allowed region intersects one of the axes at a value below 1, then the value of the corresponding coverage fraction must be less than unity (at the 1σ confidence level). Such a situation can occur if the narrow absorption doublet happens to fall on the high-velocity wing of an emission line where the underlying flux is dominated by the continuum (i.e., when W is small). Because of this technical requirement, we cannot draw any conclusions about the preferred velocity distribution of systems that cover the continuum source only partly.

Using the observed values of W from published low-resolution spectra (Sargent et al. 1988; Steidel & Sargent 1991) and the measured values of C_f we have derived constraints on the coverage fractions of the two distinct sources. These limits, along with the ingredients needed to compute them, are listed in Table 3 for each system and transition showing the signature of partial coverage. In particular, in the last two columns of Table 3 we list the range of allowed values of C_c and C_{elr} as deduced from the range of allowed solutions of equation (5). We emphasize that the limits on C_c and C_{elr} do not hold independently of each other since the solution should also satisfy equation (5). In practice these limits correspond to the extreme corners of the solution boxes as illustrated in Figure 10. The constraints on C_c and C_{elr} are also represented graphically by the vertical extent of shaded boxes and vertical bars, respectively, in Figures 6–8.

In most of the absorption components listed in Table 3, either the continuum source or the BELR could be fully covered. Notable exceptions are the SiIV line of Q 0450 – 132 and the highest-velocity component of its Nv line (at $\Delta v = -1880 \text{ km s}^{-1}$; see Figure 6), as well as the red CIV component in PG 1222 + 228 (at $\Delta v = +1587 \text{ km s}^{-1}$; see Figure 7). In these cases C_{elr} is not constrained, but the continuum source cannot be fully covered under any conditions. We derive $0.59 < C_c < 0.88$ and $C_c < 0.84$, respectively, in the case the former object and $0.12 < C_c < 0.52$ in the case of the latter object. In the Appendix we consider the possibility that the photons from the continuum source and the BELR pass through different absorbers, i.e. $\tau_c \neq \tau_{elr}$. This could be possible depending on the sizes of absorbing structures and their spatial positions relative to the emitting regions, but we show in the case of the redward component of PG 1222 + 228 partial coverage of the continuum source is required regardless of the assumed τ_c and τ_{elr} . The $\Delta v = +1587 \text{ km s}^{-1}$ component of the PG 1222 + 228 system also requires a partially covered continuum source, with a larger continuum coverage fraction. It is interesting that the range of constraints $0.51 < C_c < 0.92$ does not overlap with that of the $\Delta v = +1469 \text{ km s}^{-1}$ component.

4.3. Application of the Refined Method to Additional Quasars With Published Data

There are three other quasars with intrinsic CIV narrow line absorbers observed with HIRES/Keck I and presented in the literature in sufficient detail to derive C_f , C_c , and C_{elr} . These are PKS 0123 + 237 (radio-loud; Barlow & Sargent 1997), Q 0150–203 (UM 675; radio-quiet; Hamann et al. 1997a), and Q 2343+125 (radio-quiet; Hamann et al. 1997b). The results we obtain by applying the method of the previous section to these objects are listed in Table 4.

The NAL systems of PKS 0123 + 237 were discussed by Barlow and Sargent (1997). The velocity structure of the NAL profile of PKS 0123 + 237 is similar to that of Q 0450 – 132 but in the former object the effective coverage fraction is different for different transitions. In the case of Q 2343 + 125 (Hamann et al. 1997b) the NALs are found at a very large velocity relative to the emission-line peak ($\Delta v = -24,000 \text{ km s}^{-1}$) but still there is considerable evidence that they are intrinsic: in addition to showing the signature of partial coverage they also happen to be variable. The continuum coverage fraction can be constrained to be very small (< 0.2) because the emission-line contribution at the velocity of absorption is small ($W = 0.1$; see Table 4).

Together with the NAL systems presented in the previous section, the systems analyzed here comprise the database of available high-resolution spectra of NALs. All six intrinsic NAL systems have CIV absorption profiles with velocity widths of 100–400 km s^{-1} and have obvious sub-structure (see, for example, Figure 1). The NAL profiles suggest that there are discrete absorbing structures (though not necessarily discrete “clouds”) at different positions in velocity space.

5. Discussion

5.1. Implications of the Observational Results

Since the six quasars of Table 1 were drawn from a sample that was selected based on the properties of *intervening* MgII absorbers, they can be regarded as a collection which is unbiased towards the detection of *associated* CIV absorption lines. As such we can use it to estimate roughly how frequently associated CIV NALs are found in radio-loud and radio-quiet quasars. Associated absorption lines were detected in all three radio-quiet objects, and, in two cases, the lines were shown to be intrinsic based on the signature of partial coverage. The two NAL systems in Q 1213 – 003, which did not show the signature of partial coverage, could plausibly be intervening. One would expect to find 2 intervening systems within 5000 km s^{-1} in a sample of six quasars, based on the known density of CIV systems at $z = 2$ and the redshift path that we have observed. On the other hand, only one out of the three radio-loud objects showed an associated NAL system which also turned out to be intrinsic.

Our results are consistent with previous studies (Foltz et al. 1986; Anderson et al. 1987) that find that associated NALs are fairly common in both radio-loud and radio-quiet quasars. However, as Foltz et al. (1986) pointed out, there could be a systematic difference between the strengths of

associated NALs found in radio-loud and radio-quiet quasars. Strong NALs ($> 1.5 \text{ \AA}$) prefer radio-loud hosts, while weak NALs show no such preference. None of the five associated systems detected in our survey are strong, thus we cannot re-address this issue. It should be noted that although the associated systems that we report here are fairly weak, in three of four quasars they are still within the detection limits of the Foltz et al. (1986) and Anderson et al. (1987) surveys. However, our more sensitive survey shows that in some cases (Q 0002 + 051 and Q 1421 + 331) NALs are *not* detected down to a 5σ limit of rest-frame equivalent width, $REW < 0.05 \text{ \AA}$. This implies that there may be some lines of sight that do not pass through NAL gas.

More than 10 intrinsic NAL systems reported in the literature appear in radio-quiet quasars (Hamann et al. 1997c; Barlow et al. 1997; Tripp, Lu, & Savage 1997). It is interesting that, although Foltz et al. (1986) and Anderson et al. (1987) find associated NALs in about 70% of radio-loud quasars, only very few of these systems have been proven rigorously to be intrinsic: two systems from the sample of Foltz et al. (1986) show signs of variability (3C 205 and the “mini-BAL” in PHL 1157 + 0128; Aldcroft et al. 1997). Moreover, some fraction of associated NAL systems are bound to be intervening systems by chance; in fact 2 out of the 12 associated NAL systems in the sample of Anderson et al. (1987) are expected *a priori* to be intervening systems. A description of the properties of *intrinsic* NALs in radio-loud and radio-quiet quasars has not yet been established. A systematic survey at very high spectral resolution is needed to clarify the situation.

Another important observational result is that, in at least two quasars from our collection, the NAL gas can be demonstrated to cover the *continuum source* only partially. One of these quasars, Q 0450 – 132, is radio-quiet, while the other, PG 1222 + 228, is radio-loud. Partial coverage of the continuum source may be more common than these two cases suggest but we have no way of determining this yet. The implication of this result is not absolutely clear because the reason for the apparent partial coverage is not known. One possibility is that the absorbing medium is clumpy and the clump sizes are comparable to or smaller than the size of the continuum source. Another possibility, however, is that the continuum source is completely covered by the absorber but a scattering medium makes it possible for continuum photons to bypass the absorber and get to the observer without suffering any absorption. We expand on this issue in the next section where we consider possible explanations for the observed partial coverage.

5.2. Interpretation of Effective Partial Coverage

Central to interpreting these results is knowledge of the mechanism that can give rise to effective coverage fractions less than unity. Following our preliminary discussion of this subject in §3, three mechanisms can fill in saturated, non-black troughs, or more generally produce discrepant optical depth ratios for doublet or multiplet transitions: 1) a source function, 2) scattering of background photons back into the light path, 3) true (i.e., geometric) partial coverage of the continuum and/or BEL source by the absorbing medium. The present data do not permit us to distinguish among these possibilities, but we discuss possible tests. These tests involve polarization measurements,

consideration of the coverage fraction in different transitions, and correlating time variability with coverage fractions.

One possible source function explanation involves a non-occulted emission source which contributes additional photons to the light path after absorption of the continuum and BEL photons has occurred, essentially “diluting” the absorbed spectrum. Wampler et al. (1995) determined that an unabsorbed thermal continuum characterized by $T = 17,000$ K could explain the residual intensity in the saturated troughs of various transitions in the BAL system of Q 0059 – 2735. In fact, other intrinsic NAL systems also show variations in C_f from transition to transition, namely UM675 (Hamann et al. 1997a) and PKS 0123 + 257 (Barlow & Sargent 1997). The mechanism for production of the additional source function photons is unknown, but its contribution should vary smoothly with wavelength to produce the observed effect. Another manifestation of a source function is line emission by the same gas that is responsible for the absorption. This version of the scenario is not viable, however, since it would not have the desired effect: if there were an emission component filling in the unresolved absorption troughs it would result in an effective coverage fraction *greater than unity*.

Scattering of photons back into the light path is certainly a plausible explanation. An indirect argument for a scattering explanation is that it is known to be important in filling in the troughs of *broad* absorption lines. Spectropolarimetric observations of many BAL quasars (Ogle 1997; Brotherton et al. 1997; Cohen et al. 1995; Glenn, Schmidt, & Foltz 1994; Goodrich & Miller 1995; Hines & Wills 1995; Schmidt, Hines, & Smith 1997) show that the polarization level in saturated non-black absorption troughs is higher than in the continuum. This by no means proves that scattered light makes a large contribution for all NAL absorbers, since the lines of sight through these absorbers could well be different than in BALs. Spectropolarimetric observations of partially covered NAL systems are needed to investigate the role of scattering. Until such observations are carried out, we can consider clues provided by the relationship between time variability and partial coverage. The implications of the observational clues, however, depend on the picture that one adopts for the scatterers. If the scatterers comprise an extended collection of clumps or a quasi-uniform medium enveloping the BELR, then the scattering contribution is unlikely to vary substantially over time scales of the order of the dynamical time of the BELR gas. The strength of absorption, on the other hand, can vary as a result of changes in ionization state of the absorber or motion of the absorbing gas across the line of sight. One alternative picture is that of a discrete clump acting as a mirror to scatter continuum and/or emission-line photons in the direction of the observer without their passing through the absorber. In this picture the amount of scattered light can vary on the same time scale as the absorbing column density making a unique interpretation of the variability time scale virtually impossible. Another alternative picture is that the scatterers are close to our line of sight (they could be mixed with the absorbers or they could form a tenuous, ionized atmosphere round individual clumps in the absorber). In this case the light is scattered in the forward direction and its fractional polarization does not change. In other words, even though scattering is the culprit in this scenario, it does not betray itself by its polarization signature.

At present there is one NAL system where variability provides strong evidence *against* a scattering mechanism. The $\Delta v = -24,000$ km s $^{-1}$ CIV NAL system toward Q 2343 + 125 has an effective coverage fraction that varies substantially from one epoch of observation to another, and the effective coverage fraction is smaller when the absorption lines are weaker (Hamann et al. 1997a). This argues against a scattering picture of the above type, in which scattered light would fill in a larger fraction of the trough of a weaker line. From the time variability and the partial coverage of the continuum source for this system, Hamann et al. (1997b) derived the requirement that the absorbing clouds are quite small (~ 0.01 pc) and are located close to the continuum source. If we adopt this interpretation, then true partial coverage of the continuum source is the most plausible explanation. This suggests that time variability and true partial coverage occur together because both are related to small absorbers close to the continuum and/or BEL source. The variations can result from either motion of the clouds or from changes in the sizes of the multiphase layers of the absorber. Discriminating between these two possibilities is challenging and requires a geometric model of the absorbers and the sources of ionization, which can be constrained by observations of multiple transitions.

5.3. A General Picture of Intrinsic NALs

Narrow absorption lines are ubiquitous, appearing in all types of broad-line AGNs, namely in Seyfert 1 galaxies and broad-line radio galaxies as well as in radio-loud and radio-quiet quasars. If we take the frequency of narrow *associated* absorption lines as a rough indication of the coverage fraction of the absorbers (as seen by the continuum and/or emission-line source) then this fraction appears to be very high. It is about 50% in Seyfert 1 galaxies (Crenshaw 1997), perhaps about 70% in radio-loud quasars (Foltz et al. 1986; Anderson et al. 1987), and apparently also very high in radio-quiet quasars based on our small collection.

The observational clues available at the moment, although tantalizing, do not point clearly to a specific interpretation. Because NALs are seen in many different types of active galaxies and seem to be quite common, their relation to BALs is unclear. Unlike BALs, NALs are common in radio-loud quasars and in Seyfert 1's. It is plausible that NALs with large velocities and those that are quite broad and without structure (“mini-BALs”) are related to the BAL phenomenon (Hamann et al. 1997c). This hypothesis is supported by the fact that large outflow velocities ($>10,000$ km s $^{-1}$), such as in Q 2343 + 125, Q 0935 + 417 (Hamann et al. 1997c), and Q 1700 + 64 (Tripp et al. 1997), have only been observed in radio-quiet quasars, as have the majority of BALs. Radio-loud quasars on the other hand have mostly narrow, “associated” absorption lines. Finally, associated NALs found in Seyfert 1 galaxies show limited observational evidence for an intrinsic nature. Some have covering factors close to unity (Crenshaw 1997), and in two cases, NGC 3783 and NGC 3516, the NALs vary on a short time scale (Koratkar et al. 1996; Shields & Hamann 1997). Interestingly enough NALs in Seyfert 1 galaxies are always blueshifted relative to the BELs, unlike NALs in quasars which are sometimes redshifted relative to the BELs. Based on the above summary,

a reasonable model or scenario for the NAL gas should explain why NALs are so common (in other words, why the absorbing gas covers such a large solid angle relative to the continuum source) and why they are sometimes observed to be redshifted and sometimes blueshifted relative to the peaks of the broad emission lines (i.e. apparent infall as well as outflow).

It is obviously impossible to construct a unique unifying model to explain these observational facts. Nevertheless, we venture to speculate on how NALs can fit into the accretion-disk wind picture of Murray et al. (1995), which was originally meant to explain BALs. Their possible relatives, the high velocity NALs, could originate in a different phase of the same region or in an atmosphere just outside the wind. Sometimes both NALs and BALs arise in the same quasar, at different velocities, so it seems plausible that NAL phases could exist nearby the BAL region. The broader, smoother, mini-BALs may also be related to this type of wind flow. In this context, it is extremely interesting that in some cases the NALs are redshifted relative to the *broad* emission-line peak. Of course this relative redshift does not necessarily imply infall towards the central engine. The systemic redshift is best determined from the *narrow* emission lines, which, however, have not been observed in these particular objects. Because the peaks of the broad emission lines can be blueshifted relative to the systemic redshift, it is possible that the observed NALs are also blueshifted relative to the systemic redshift. At any rate, all four of the NAL systems in radio-loud quasars that have been demonstrated to be intrinsic, i.e., PG 1222+228 (this paper), Q 0123+237 (Barlow & Sargent 1997), 3C 205 (Aldcroft et al. 1997), and PHL 1157+014 (Aldcroft et al. 1997), have NALs that *appear to be* redshifted with respect to the peaks of the broad emission lines. In Figure 11, we show schematically a side view of the geometry of the accretion-disk wind of Murray et al. (1995) and a plausible location for the NAL gas. For specific orientations of the observer (such that $\beta < i$, where i is the inclination of the disk relative to the observer and β is the opening angle of the wind, as shown in the figure), the NALs originating in the far side of the disk can appear redshifted, assuming that the NAL gas is outflowing. Since the NALs are sometimes deeper than the net emission-line level on which they are superposed, the absorbing gas must intercept continuum photons as well. To accommodate such an effect in this picture we must postulate that the outflowing NAL gas originates very close to the center of the disk so that it can cover the continuum source, i.e., it fills the region between the fast disk wind and the disk axis. We emphasize, however, that alternative pictures are also plausible. For example, the NAL gas could be located on the near side of the disk, in the direction of the observer. Because the wind is rotating as well as outflowing, the net velocity vector of the outflowing gas can point away from the observer depending on the azimuth, in which case the resulting absorption lines will also appear redshifted.

In the context of the speculative geometric picture outlined above, the difference between AGN subclasses may be related to the properties of the fast wind. For example, if the opening angle of the wind is very small, the wind effectively “hugs” the accretion disk and the likelihood of our line of sight going through it is very small. Hence BALs would not be observed in such objects but NALs could still appear. We speculate further that the difference between radio-quiet quasars on one hand and radio-loud quasars and Seyferts on the other is the opening angle of the wind,

which may in turn be a consequence of the luminosity of the object (relative to the Eddington luminosity), of the shape of the ionizing continuum, or of the combination of these two properties. This could also affect the strength of NALs in the two cases as observed by Foltz et al. (1986) for radio-loud vs. radio quiet quasars. Finally, we note that if any hot electrons happen to be located in the direction of the axis of the disk, they can act as scatterers and redirect continuum photons towards the observer. Through this effect, the absorption lines can be “diluted” creating the impression that the absorber only partly covers the continuum source.

6. Summary and Conclusions

In this paper we reported the discovery of five narrow “associated” ($|\Delta v| < 5000 \text{ km s}^{-1}$) absorption-line systems in the spectra of four quasars. These quasars were observed in the course of a survey for intervening MgII absorbers, in which the CIV emission lines of six objects happened to fall in the observed spectral range. As such, this “mini-sample” of six quasars is unbiased towards the presence of narrow, intrinsic CIV absorption lines. Three of the absorption systems were demonstrated to be intrinsic, because the relative strengths of the members of the CIV doublet required effective partial coverage of the continuum and/or emission-line sources. The two systems toward Q 1213 – 003 could not be demonstrated as intrinsic because their coverage fractions were consistent with unity.

We carried out a detailed analysis of the coverage fractions of the three intrinsic systems that we have found: Q 0450 – 132, PG 1222 + 228, and PG 1329 + 412. The analysis consisted of determining the effective coverage fraction of the background source(s) by the absorber according to the method of Barlow & Sargent (1997) as well as a refinement of this method to treat the coverage fractions of the background continuum and emission-line sources separately. The latter technique was also applied to three additional intrinsic NAL systems for which sufficient information was available in the literature: PKS 0123+237, UM 675, and Q 2343+125. This provided a total of six intrinsic NAL systems studied at high resolution, and among the six there was a very wide range of properties. The derived CIV effective coverage fractions ranged from $C_f \sim 0.1$ to nearly unity, and in some systems varied across the absorption profiles. The velocities of the absorbing clouds, relative to the quasar, ranged from outflow at $24,000 \text{ km s}^{-1}$ to apparent infall at 1500 km s^{-1} . In three systems, Q 0450 – 132 and PG 1222 + 228 (this study) and Q 2343 + 125 (Hamann et al. 1997b), the data require that the covering factor of the *continuum* source is less than unity ($C_c < 1$, according to our formulation presented in §4.2). The two systems are quite different from each other: Q 2343 + 125 is radio-quiet and its absorption system is at an outflow velocity of $24,000 \text{ km s}^{-1}$, while PG 1222 + 228 is radio-loud and its absorption system is redshifted relative to the BEL region by 1500 km s^{-1} .

We have discussed mechanisms which can give rise to a covering factor that is less than unity but we have not been able to select a favorite based on the information that is currently available from observations. We have also speculated that the NAL gas may be related to the fast outflows

that manifest themselves as BALs. If this is indeed the case, then the fact that NALs are quite common in radio-loud quasars and in Seyfert 1 galaxies may imply that these types of AGN also harbor fast accretion-disk winds, whose absorption signature (BAL) is unobservable. Further observations, and more specifically systematic surveys of the various classes of active galaxies and quasars, are needed to test these ideas. Some of the key goals of these surveys should be to: 1) establish just how common *intrinsic* NALs are in radio-loud/quiet quasars and in Seyfert 1's; and 2) check if non-unity covering factor and time variability occur together as a clue toward understanding the spatial distribution of the NAL clouds. In addition spectropolarimetric observations are sorely needed to establish whether scattering or true partial coverage by small absorbers is responsible for effective covering factors less than unity.

We thank Jules Halpern as well as the anonymous referee for useful suggestions. This work was supported by the National Science Foundation Grants AST-9529242 and AST-9617185, and by NASA Grant NAG5-6399. During the early stages of this work M.E. was based at the University of California, Berkeley and was supported by a Hubble Fellowship (grant HF-01068.01-94A from Space Telescope Science Institute, which is operated for NASA by the Association of Universities for Research in Astronomy, Inc., under contract NAS 5-26255). We are grateful to Steven S. Vogt for the great job he did building HIRES.

APPENDIX

A. More General Forms of the Partial Coverage Calculation

Here we consider the consequences of two simplifying assumptions that we made in the calculation of the coverage fraction in §4.2: (1) the emission line flux is the same for both members of the doublet; and (2) the optical depths toward the continuum source and the BLR are the same.

A.1. Underlying Emission-Line Flux Differs from Stronger to Weaker Transition

We have assumed that the ratio of the emission line to the continuum flux is the same in the blue and red components of a doublet, i.e. that $W_b = W_r = W$. This assumption may lead to inaccuracies in the derivation of the coverage fraction when the absorption falls on the steep part of an emission feature so that W_b and W_r may differ by 10–15%. In this more general case we have

$$\frac{(1 - R_b)(1 + W_b)}{C_c + W_b C_{elr}} = \frac{2(1 - R_r)(1 + W_r)}{C_c + W_r C_{elr}} - \left[\frac{(1 - R_r)(1 + W_r)}{C_c + W_r C_{elr}} \right]^2 , \quad (A1)$$

which can be reduced to a quadratic equation in C_{elr} if C_c is specified (or in C_c if C_{elr} is specified).

To see how the assumption used previously will affect our results, consider the quasar Q 0450–

132 which has its absorption on the steepest area of its emission feature. In this case, using $W_r = 0.83$ and $W_b = 0.7$ changes C_c or C_{elr} only by 12 – 15%.

A.2. Different Absorbers Cover Continuum and BEL Sources

Here we examine the more general case of incomplete coverage of the two distinct sources of photons (continuum source and BEL) where the light from the two sources is allowed to pass through different absorbing clouds (or significantly different regions of the same cloud). Let τ_c and τ_{elr} be the optical depths along the lines of sight from observer to continuum source and from observer to BEL source. If the clouds occult a fraction C_c and a fraction C_{elr} of the lines of sight toward each source, then the normalized residual intensity is:

$$R = \frac{(1 - C_c) + C_c e^{-\tau_c} + (1 - C_{elr})W + C_{elr}W e^{-\tau_{elr}}}{(1 + W)} , \quad (A2)$$

where W is the emission line flux in continuum units. In conjunction with optical depth scaling laws, this gives a system (for an n -transition multiplet) of $3n - 2$ equations (n residual intensity equations, $n - 1$ continuum optical depth relations, $n - 1$ ELR optical depth relations) and $2(n + 1)$ unknowns (2 coverage fractions and $2n$ optical depths). This can, in principle, be solved for a multiplet with at least four transitions.

With this more general case in mind we now reconsider the issue of partial coverage of the continuum source in PG 1222 + 228 to see if this interesting result still applies. At the position of the $\Delta v = +1587 \text{ km s}^{-1}$ component of the CIV absorption (Figure 4) the continuum contributes $\sim 77\%$ of the total flux (i.e., $W = 0.3$), and the BELR only 23%. The observed flux at that position is 0.6 in normalized units. Therefore it is not possible to have zero coverage of the continuum source because then the observed flux would be *at least* 0.77 no matter what the values of C_{elr} and τ_{elr} . If $C_c = 1$ then $0.24 < \tau_c(\lambda 1550) < 0.73$. The lower limit is provided by the requirement that the continuum photons alone (those that pass through the absorber) do not produce too much flux. The upper limit is the minimum contribution from unimpeded continuum photons since the BEL can contribute at most a flux of 0.3. Over that range of τ_c , the continuum photons that pass through the absorber produce a flux ranging from 0.6 to 0.3 at the position of CIV $\lambda 1550$ and from 0.48 to 0.18 at the position of CIV $\lambda 1548$. In either case, the *observed* flux at 1548 Å is just slightly smaller than at 1550 Å (0.60 as compared to 0.62). To be consistent with these data, the contribution to the flux from the BEL photons would have to be larger at 1548 Å than at 1550 Å. The contribution from photons that do not pass through absorbers is the same for the two transitions, and the contribution from photons at 1550 Å that make it through the absorber should be equal or larger than at 1548 Å. This is the opposite of what is required. Thus the continuum source cannot be fully covered at any τ_c . Since $C_c \neq 0$ and $C_c \neq 1$ we conclude that the continuum source must be partially covered regardless of assumptions about τ_c and τ_{elr} .

REFERENCES

Aldcroft, T., Bechtold, J., & Foltz, C. 1997, in "Mass Ejection from Active Galactic Nuclei," ASP Conference Series 128, eds. N. Arav, I. Shlosman, & R. Weymann (San Francisco: ASP), 25

Anderson, S. F., Weymann, R. J., Foltz, C. B., & Chaffee, F. H. 1987, AJ, 94, 278

Arav, N., Korista, K. T., Barlow, T. A., & Begelman, M. C. 1995, Nature, 376, 576

Barlow, T. A., Hamann, F., & Sargent, W. L. W., 1997, in "Mass Ejection from Active Galactic Nuclei," ASP Conference Series 128, eds. N. Arav, I. Shlosman, & R. Weymann (San Francisco: ASP), 13

Barlow, T. A. & Sargent, W. L. W. 1997, AJ, 113, 136

Barvainis, R., Lonsdale, C., & Antonucci, R. 1996, AJ, 111, 1431

Becker, R. H., Gregg, M. D., Hook, I. M., McMahon, R. G., White, R. L., & Helfand, D. J. 1997, ApJ, 497, L93

Becker, R. H., White, R. L., & Helfand, D. J. 1995, ApJ, 450, 559

Brotherton, M. S., Tran, H. D., van Breugel, W., Dey, A., & Antonucci, R. 1997, ApJ, 487, L113

Brotherton, M. S., van Breugel, W., Smith, R. J., Boyle, B. J., Shanks, T., Croom, S. M., Miller, L., & Becker, R. H. 1998, ApJ, 505, L7

Churchill, C. W. 1997, Ph.D. Thesis, University of California, Santa Cruz

Churchill, C. W., Rigby, J. R., Charlton, J. C., & Vogt, S. S. 1998, ApJS, in press (astro-ph/9807131)

Cohen, M. H., Ogle, P. M., Vermeulen, R. C., Miller, J. S., Goodrich, R. W., & Martel, A. R. 1995, ApJ, 447, L77

Condon, J. J., Cotton, W. D., Greisen, E. W., Yin, Q. F., Perley, R. A., & Taylor, G. B. 1998, ApJ, 115, 1693

Crenshaw, D. M. 1997, in "Mass Ejection from Active Galactic Nuclei," ASP Conference Series 128, eds. N. Arav, I. Shlosman, & R. Weymann (San Francisco: ASP), 121

Crenshaw, D. M., Maran, S. M., & Mushotzky, R. F. 1998, ApJ, 496, 797

Drew, J. E. 1990 in "Physics of Classical Novae," IAU Colloq. 122, eds. A. Cassatella & R. Viotti (Berlin: Springer-Verlag), 228

Elvis, M., et al. 1994, ApJS, 95, 1

Foltz, C. B., Weymann, R. J., Sun, L., Malkan, M. A., & Chaffee, F. H. 1986, ApJ, 307, 504

George, I. M., Turner, T. J., Netzer, H., Nandra, K., Mushotzky, R. F., & Yaqoob, T. 1998, ApJS, 114, 73

Glenn, J., Schmidt, G. D., & Foltz, C. B. 1994, ApJ, 437, L47

Goodrich, R. W. & Miller, J. S. 1995, ApJ, 448, L73

Gregory, P. C. & Condon, J. J. 1991, ApJS, 75, 1011

Hamann, F., Barlow, T. A., Junkkarinen, V., & Burbidge, E. M. 1997a, ApJ, 478, 80

Hamann, F., Barlow, T. A., & Junkkarinen, V. 1997b, ApJ, 478, 87

Hamann, F., Barlow, T. A., Cohen, R. D., Junkkarinen, V., & Burbidge, E. M., 1997c, in "Mass Ejection from Active Galactic Nuclei," ASP Conference Series 128, eds. N. Arav, I. Shlosman, & R. Weymann (San Francisco: ASP), 19

Hamann, F., Cohen, R. D., Shields, J. C., Burbidge, E. M., Junkkarinen, V., & Crenshaw, D. M. 1998, ApJ, 496, 761

Hines, D. C. & Wills, B. J. 1995, ApJ, 448, L69

Kellermann, K. I., Sramek, R. A., Schmidt, M., Green, R. F., & Shaffer, D. B. 1994, AJ, 108, 1163

Koratkar, A. et al. 1996, ApJ, 470, 378

Krolik, J. H. & Kriss, G. A. 1995, ApJ, 447, 512

Lanzetta, K. M., Turnshek, D. A., & Wolfe, A. M. 1987, ApJ, 322, 739

Mauche, C. 1994, in "Interacting Binary Stars," ASP Conf. Ser. 56, ed. A. W. Shafter (San Francisco: ASP), 74

Murray, N., Chiang, J., Grossmann, S. M., & Voit, G. M. 1995, ApJ, 454, L105

Ogle, P. M. 1997, in "Mass Ejection from Active Galactic Nuclei," ASP Conference Series 128, eds. N. Arav, I. Shlosman, & R. Weymann (San Francisco: ASP), 78

Petitjean, P., Rauch, M., & Carswell, R. F. 1994, A&A, 291, 29

Reynolds, C. S. 1997, MNRAS, 286, 513

Sargent, W. L. W., Boksenberg, A., & Steidel, C. C. 1988, ApJS, 68, 539

Savage, B. D., Sembach, K. R. 1991, ApJ, 379, 245

Schmidt, G. D., Hines, D. C., & Smith, P. S. 1997, in “Mass Ejection from Active Galactic Nuclei,” ASP Conference Series 128, eds. N. Arav, I. Shlosman, & R. Weymann (San Francisco: ASP), 106

Shields, J. C., Ferland, G. J., & Peterson, B. M. 1995, ApJ, 441, 507

Shields, J. C. & Hamann, F. 1997, ApJ, 481, 752

Sowinski, L. G., Schmidt, G. D., & Hines, D. C. 1997, in “Mass Ejection from Active Galactic Nuclei,” ASP Conference Series 128, eds. N. Arav, I. Shlosman, & R. Weymann (San Francisco: ASP), 305

Steidel, C. C., & Sargent, W. L. W. 1991, ApJ, 382, 433

Stocke, J. T., Morris, S. L., Weymann, R. J., & Foltz, C. B. 1992, ApJ, 396, 487

Tripp, T. M., Lu, L., & Savage, B. D. 1997, ApJS, 112, 1

Turnshek, D. A., Foltz, C. B., Grillmair, C. J., & Weymann, R. J. 1988, ApJ, 325, 651

Vogt, S. S., et al. 1994, SPIE, 2198, 326

Wampler, E. J., Bergeron, J., & Petitjean, P. 1993, A&A, 273, 15

Wampler, E. J., Chugai, N. N., & Petitjean, P. 1995, ApJ, 443, 586

Weymann, R. J., Morris, S. L., Foltz, C. B., & Hewett, P. C. 1991, ApJ, 373, 23

White, R. L. & Becker, R. H. 1992, ApJS, 79, 331

Young, P., Sargent, W. L. W., & Boksenberg, A. 1982, ApJS, 48, 455

Table 1. Summary of Quasars Properties

Object	Other Names	z_{em}^{a}	m_V (mag)	$P_{5 \text{ GHz}}^{\text{b}}$ (W Hz $^{-1}$)	R^{c}	Radio Class	Ref. $^{\text{d}}$
Q 0002 + 051	UM018, PHL 0650	1.899	16.2	2×10^{27}	110	loud	1,2
Q 0450 – 132		2.253	17.5	$< 4 \times 10^{25}$	< 5	quiet	3
Q 1213 – 003	UM485	2.691	17.0	$< 5 \times 10^{25}$	< 3.5	quiet	3
PG 1222 + 228	Ton 1530	2.040	15.5	1×10^{26}	3.8	loud	4,5
PG 1329 + 412		1.937	16.3	5×10^{24}	0.3	quiet	4
Q 1421 + 331	Mrk 679	1.906	16.7	2×10^{26}	17	loud	6

^aEmission redshift as determined from the peak of the broad CIV emission line (Sargent et al. 1988; Steidel & Sargent 1991)

^bRadio power at a rest frequency 5 GHz (see text in §2 for more details).

^cRatio of rest-frame 5 GHz-to-4400 Å flux densities.

^dREFERENCES TO RADIO OBSERVATIONS.— (1) 87GB survey; Gregory & Condon 1991; (2) White & Becker 1992; (3) NVSS survey; Condon et al. 1998; (4) Kellermann et al. 1994; (5) Barvainis, Lonsdale, & Antonucci 1996; (6) FIRST survey; Becker, White, & Helfand 1995

Table 2. Observation Log and Absorption Line Properties

Object	Observation Log			Absorption-Line Properties		
	UT Date ^a	Exposure (s)	λ Range (Å)	Δv ^b (km s ⁻¹)	REW ^c (Å)	EW_{\min} ^d (mÅ)
Q 0002 + 051	1994 Jul 5	2700	3656–6079	50
Q 0450 – 132	1995 Jan 24	5400	3987–6425	–2011	1.028 ± 0.006	30
Q 1213 – 003	1995 Jan 24	5200	5008–7357	–1566	0.108 ± 0.003	11
				–60	0.149 ± 0.004	13
PG 1222 + 228	1995 Jan 23	3600	3811–6305	+1482	0.268 ± 0.005	17
PG 1329 + 412	1996 Jul 18	6300	3766–5791	+314	0.371 ± 0.009	51
Q 1421 + 331	1995 Jan 23	3600	3819–6317	50

^aThe 1996 July exposures were severely affected by cloud cover.

^bVelocity offset of the centroid of the CIV associated absorption profile (Sargent et al. 1988; Steidel & Sargent 1991). A negative value denotes a blueshift.

^cThe rest-frame equivalent width of the CIV $\lambda 1548$ absorption line.

^dThe minimum measurable equivalent width (5σ limit; Lanzetta et al. 1987) in the velocity range of interest.

Table 3. Coverage Fractions Averaged over Small Velocity Bins^a

Ion	$\langle v \rangle^b$ (km s ⁻¹)	C_f	W	C_c^c	C_{elr}^c
Q 0450 – 132					
CIV	–2109	0.83 ± 0.02	0.75 ± 0.02	> 0.65	> 0.53
	–2057	0.61 ± 0.08		> 0.35	> 0.10
	–2014	0.93 ± 0.02		> 0.83	> 0.72
	–1940	0.75 ± 0.06		> 0.45	> 0.22
	–1870	0.68 ± 0.10		> 0.24	unconstrained
SiIV	–2108	0.72 ± 0.08	0.10 ± 0.02	0.59–0.88	unconstrained
Nv	–2051	0.48 ± 0.24	0.50 ± 0.02	unconstrained	unconstrained
	–2013	0.85 ± 0.06		> 0.68	> 0.16
	–1948	0.69 ± 0.29		> 0.09	unconstrained
	–1880	0.36 ± 0.20		< 0.84	unconstrained
PG 1222 + 228					
CIV	+1469	0.67 ± 0.04	0.30 ± 0.02	0.51–0.92	unconstrained
	+1587	0.36 ± 0.04		0.12–0.52	unconstrained
PG 1329 + 412					
CIV	+273	0.81 ± 0.04	0.70 ± 0.02	> 0.60	> 0.40
	+311	0.55 ± 0.53		unconstrained	unconstrained
	+336	0.89 ± 0.17		> 0.52	> 0.14
	+365	0.67 ± 0.09		> 0.29	unconstrained

^aThis table gives the weighted-mean coverage fractions of detected NALs, averaged over small velocity bins of width 20–40 km s⁻¹. Each bin is labelled by its mean velocity.

^bThe reported values of C_f and $\langle v \rangle$ are weighted averages over the listed velocity range. Weights were assigned according to the variance in each resolution element's computed coverage fraction.

^cThe range of allowed values of C_c and C_{elr} based on the measured values of C_f and W . The limits are determined by applying equation (5) and using the 1σ uncertainties on the measured quantities. They correspond to the corners of the extreme boxes of allowed solutions similar to those illustrated in Figure 10. As such they cannot hold independently of each other because the solution must also satisfy equation (5).

Table 4. Coverage Fractions from Literature

Ion	$\langle v \rangle$ (km s ⁻¹)	W	C_f	C_c^a	C_{elr}^a
Q 0123 + 237 (radio loud; Barlow & Sargent 1997)					
CIV	+190	1.0	$0.63^{+0.07}_{-0.04}$	>0.26	>0.26
CIV	+480	1.0	$0.94^{+0.04}_{-0.03}$	>0.88	>0.88
NV	+190	0.3	$0.79^{+0.21}_{-0.17}$	>0.73	>0.09
NV	+480	0.3	$0.98^{+0.02}_{-0.02}$	>0.98	>0.93
SiIV	+480	0.2	$0.93^{+0.07}_{-0.05}$	>0.92	>0.57
Ly α	+190	0.9	>0.91	>0.80	>0.80
Ly α	+480	0.9	>0.85	>0.71	>0.68
Q 0150 – 203 (radio quiet; Hamann et al. 1997a)					
CIV	-1520	1.2	$0.46^{+0.1}_{-0.0}$	unconstrained	<0.80
CIV	-1400	1.1	$0.44^{+0.1}_{-0.0}$	<0.97	<0.80
NV	-1700	0.8	$0.32^{+0.3}_{-0.0}$	<0.58	<0.72
NV	-1520	0.8	$0.63^{+0.2}_{-0.1}$	>0.33	>0.17
NV	-1400	0.8	$1.00^{+0.0}_{-0.1}$	1.00	1.00
NV	-1300	0.8	$1.00^{+0.0}_{-0.1}$	1.00	1.00
Q 2343 + 125 (radio quiet; Hamann et al. 1997b)					
CIV	-24,000 ^b	0.1	$0.045^{+0.03}_{-0.00}$	<0.50	<0.50
CIV	-24,000 ^c	0.1	$0.19^{+0.04}_{-0.02}$	0.11–0.21	unconstrained

^aThe limits on C_c and C_{elr} have the same significance as in Table 3.

^bAs observed in 1994 September.

^cAs observed in 1995 October.

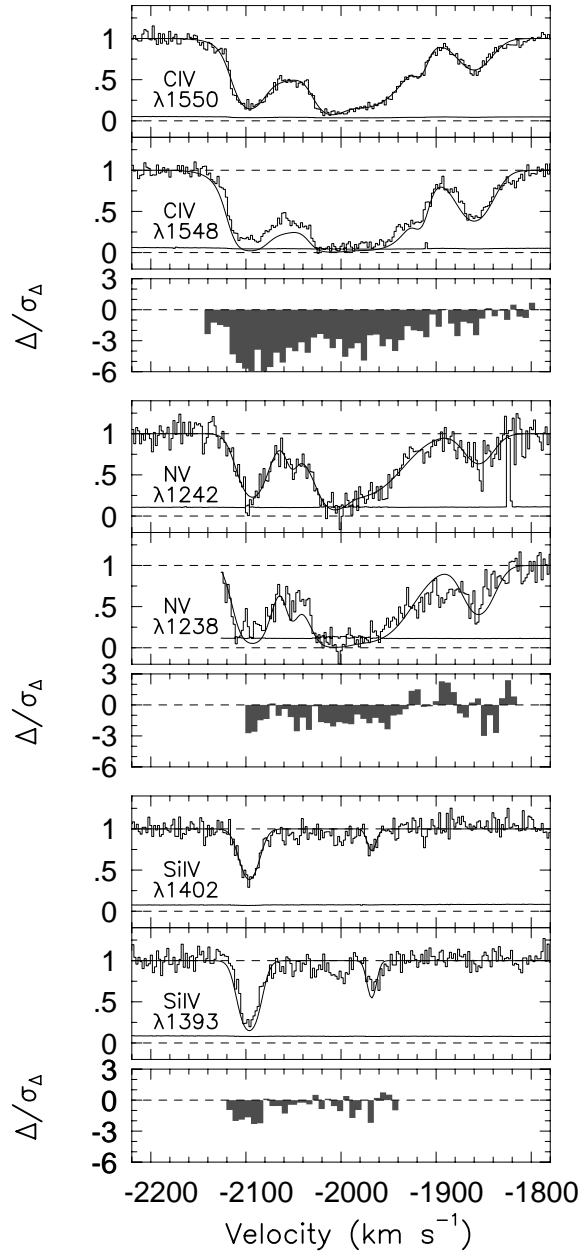


Fig. 1.— Velocity-aligned normalized flux profiles of detected transitions in the $\Delta v = -2011 \text{ km s}^{-1}$ NAL system toward Q 0450 – 132. Model fits to the weaker doublet members (panels 1, 4, and 7 from the top) are shown as solid curves superimposed on the spectra. The optical depth of each model component is scaled according to atomic physics and overplotted on the stronger transitions (panels 2, 5, and 8). Panels 3, 6, and 9 show the apparent deviations of the optical depths from the predicted value averaged over a resolution element and scaled by the error bar. The CIV doublet in this particular system clearly shows inconsistencies in the optical scaling and is indicative of partial coverage.

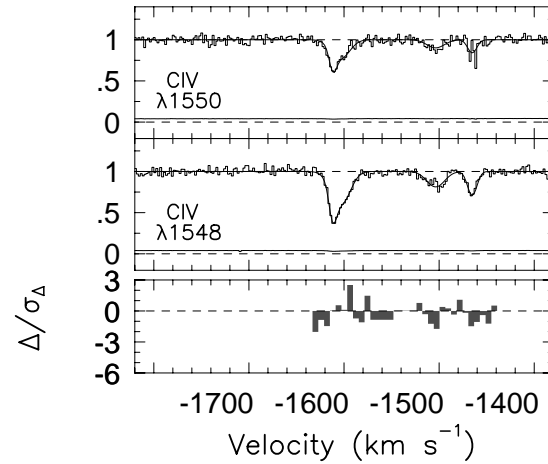


Fig. 2.— Same as Figure 1, but for the $\Delta v = -1566$ km s⁻¹ system toward Q 1213 – 003.

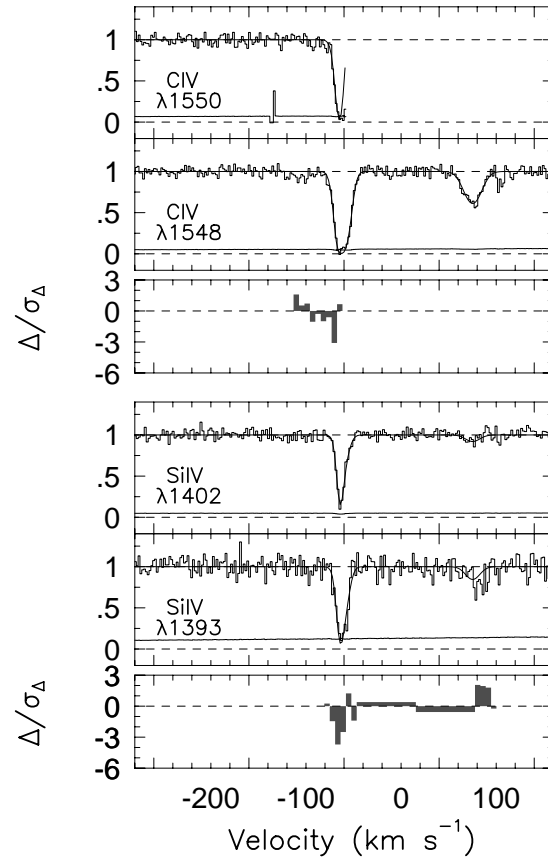


Fig. 3.— Same as Figure 1, but for the $\Delta v = -60 \text{ km s}^{-1}$ system toward Q 1213 – 003.

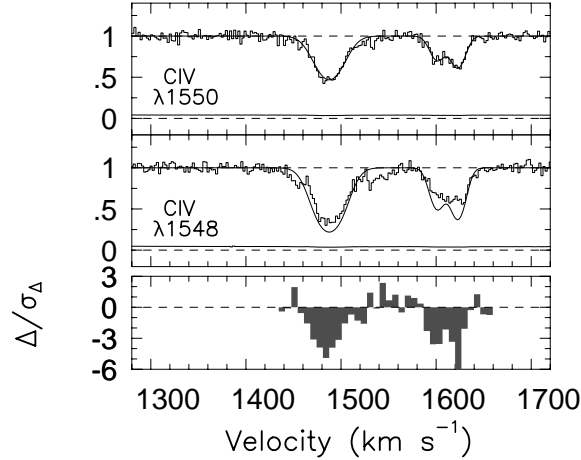


Fig. 4.— Same as Figure 1, but for the $\Delta v = +1482 \text{ km s}^{-1}$ system toward PG 1222 + 228. The obvious discrepancy between the atomic physics prediction and the data in this particular case is indicative of partial coverage.

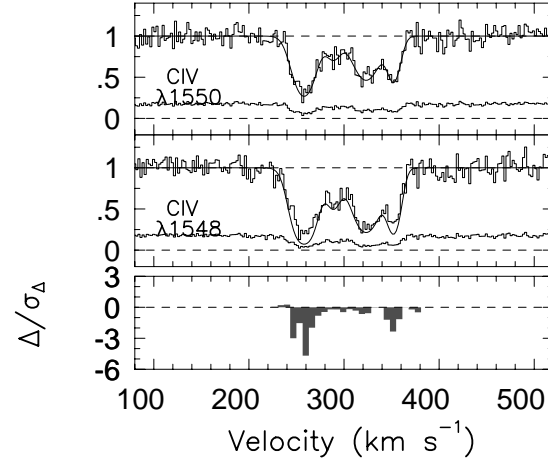


Fig. 5.— Same as Figure 1, but for the $\Delta v = +314 \text{ km s}^{-1}$ system toward PG 1329 + 412. The obvious discrepancy between the atomic physics prediction and the data in this particular case is indicative of partial coverage.

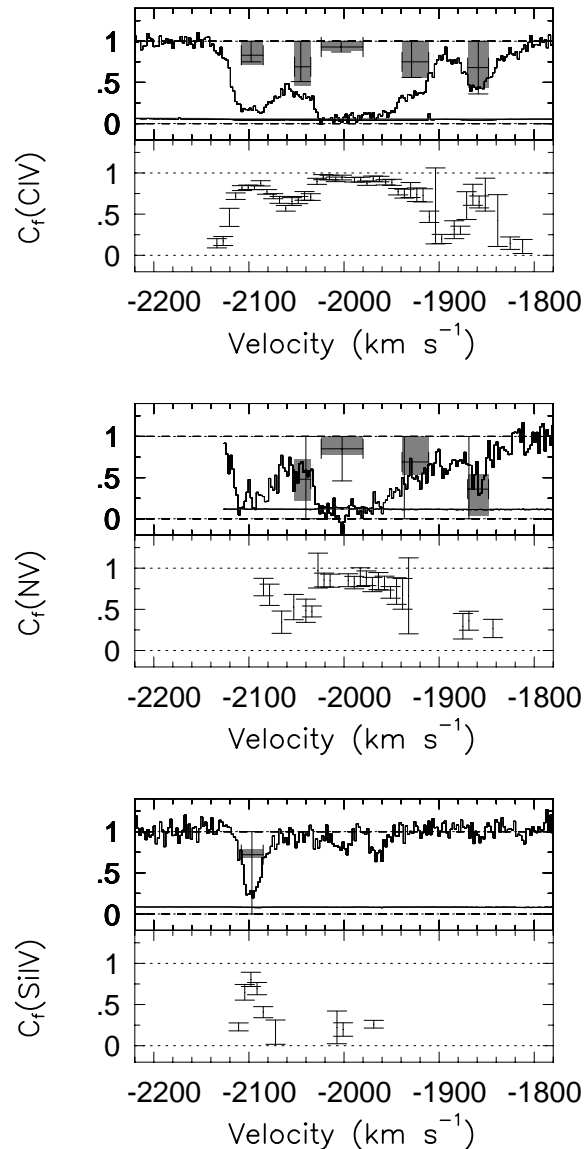


Fig. 6.— For each detected species in the Q 0450–132 intrinsic NAL system, the effective coverage fraction profile, $C_f(v)$, with 1σ error bars is shown in the bottom windows of each panel. In the top windows, the line profiles are shown for reference along with a graphical representation of the emission-line region and continuum source coverage fractions averaged over 20–40 km s^{-1} –wide velocity bins. The level of the horizontal bars represents the weighted-mean C_f computed over a velocity range given by its width. The vertical bar intersects the horizontal bar at the weighted-mean velocity and represents the allowed coverage fraction range for the emission line region. The allowed coverage fraction ranges for the continuum are given by the vertical extent of the shaded boxes. See §4.2.

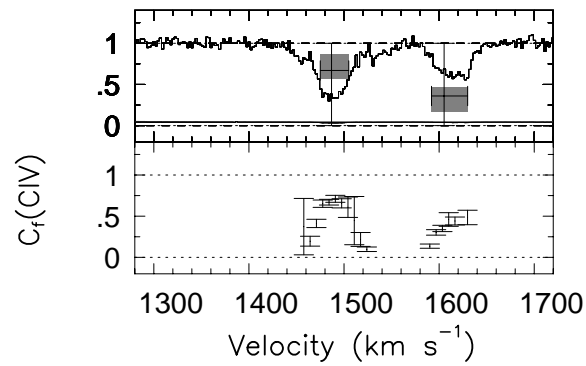


Fig. 7.— Same as Figure 6, but for the PG 1222 + 228 intrinsic system.

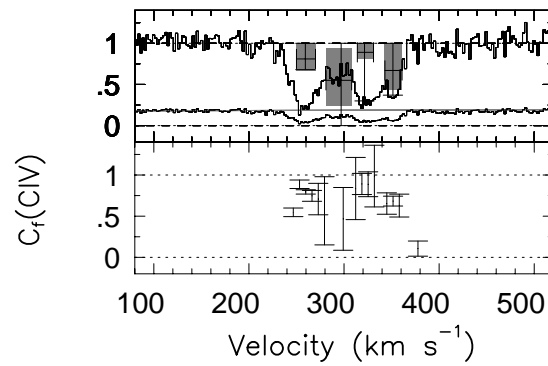


Fig. 8.— Same as Figure 6, but for the PG 1329 + 412 intrinsic system.

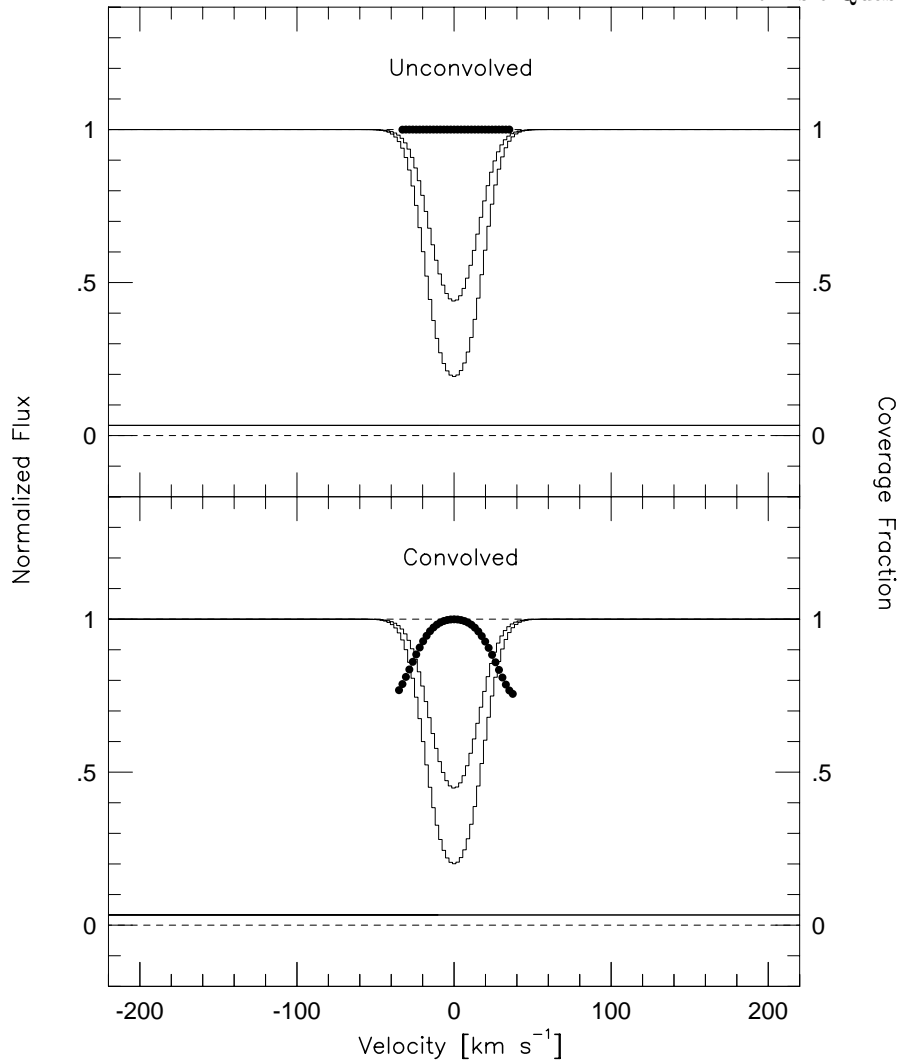


Fig. 9.— Convolution with the instrument's line spread function affects the computation of the effective coverage fraction profile, $C_f(v)$, more in the wings of components than in their cores. The two windows show simulated flux profiles of the CIV doublet at infinite signal-to-noise ratio, but finite sampling, along with the coverage fraction derived from them (plotted as a series of circles). The top window shows the theoretical profiles before convolution with the instrumental line-spread function. The coverage fraction derived from them is unity at all velocities. However, when convolved with the HIRES/Keck I instrumental profile ($R \sim 6.6 \text{ km s}^{-1}$) (bottom window), the wings are smeared out and the original line ratio in the wings is distorted. As a result the coverage fraction measured in the wings is falsely determined to be less than unity. For more details see §4.1 of the text.

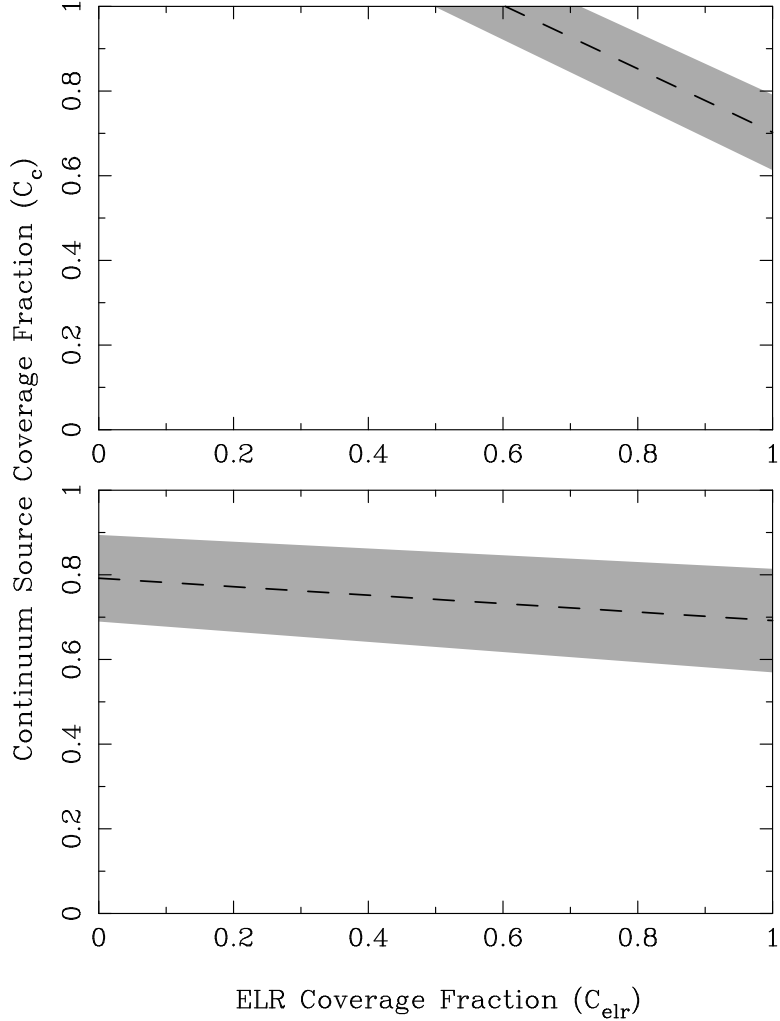


Fig. 10.— The C_c – C_{elr} parameter plane showing the solutions allowed by equation (5). Given the measured values of the effective coverage fraction, C_f , and the local line-to-continuum flux ratio, W , equation (5) implies a relation between C_c and C_{elr} . Two examples of such a relation are plotted in the two panels of this figure; they are described by $C_f = 0.83 \pm 0.02$, $W = 0.75 \pm 0.02$ and $C_f = 0.72 \pm 0.08$, $W = 0.10 \pm 0.02$, respectively. The thick dashed lines show the relation implied by the nominal values of the measured parameters. Because of the uncertainties in the measured parameters the allowed solution is not confined to the line but it can lie anywhere within the shaded box.

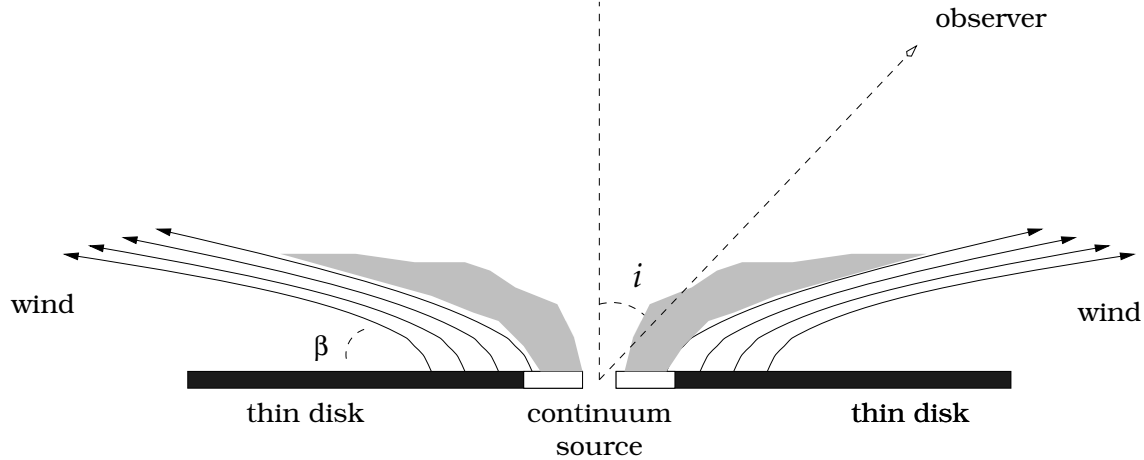


Fig. 11.— A schematic illustration of the geometry of the fast (BAL) accretion-disk wind of Murray et al. (1995) and a plausible location of the NAL gas (grey-shaded region). The arrows show the streamlines of the fast wind. The NAL gas could form an atmosphere or an interface between the fast wind and the surrounding medium (indicated in grey). The observer's line of sight is inclined at an angle i relative to the axis of the disk, while the opening angle of the fast wind relative to the disk plane is β . If the NAL gas is outflowing along with the fast wind and is seen in absorption against it, then the NALs from the far side of the outflow will appear redshifted to the observer if $\beta < i$.